INORGANIC CHEMISTRY FRONTIERS

RESEARCH ARTICLE

View Article Online
View Journal

Cite this: DOI: 10.1039/d5qi00311c

Tailoring high-entropy borides for hydrogenation: crystal morphology and catalytic pathways†

Abraham A. Rosenberg,[a] Daniel T. Lintz,[a] Juncheng Li,[a,b] Yiren Zhang,[a] Joseph T. Doane,[a] Miranda N. Bristol,[a] Alma Kolakji,[a] Ting Wang *[a,b] and Michael T. Yeung *[a]

Received 30th January 2025,
Accepted 8th April 2025

DOI: 10.1039/d5qi00311c

rsc.li/frontiers-inorganic

The high-entropy boride (HEB) $Al_{0.2}Nb_{0.2}Pt_{0.2}Ta_{0.2}Ti_{0.2}B_2$, with its unique crystal structure and high coordination (platinum coordinated to 12 boron atoms), has been shown in our previous work to exhibit exceptional catalytic properties, especially in sulfur-rich environments, where traditional platinum catalysts would succumb to sulfur poisoning. In this work, we investigate the mechanism of the HEB catalyst, first by comparing the synthesis by flux growth, as previously reported, to an arc-melting preparation. It is evident that the aluminum flux growth synthesis encourages the growth of single crystals, with clear and defined crystal facets, whereas the arc-melted sample exhibits poorly defined facets with non-uniform morphology. Here, we explore two potential mechanisms: hydrogen spillover effect (HSPE) and hydrogen atom transfer (HAT), by which the catalytic pathway is performed. Hydrogenation reactions were performed using WO_3 and 2,2,6,6-tetramethyl-1-piperidinyloxyl (TEMPO), which highlight the ability of the heterogeneous HEB catalyst to perform hydrogenation through a suspended solid solution in addition to a dissolved solution. We propose that the HEB $Al_{0.2}Nb_{0.2}Pt_{0.2}Ta_{0.2}Ti_{0.2}B_2$ follows a hybrid HAT/HSPE mechanism, where H_2 binds to the platinum atoms on the edges of the HEB and dissociates, and then the radical hydrogen departs to the substrate.

Introduction

Catalysis is vital to our modern world, and it contributes to more than 35% of the global GDP, being the cornerstone of many industrial processes, where 80% of manufactured goods involve catalysis at some point in their processing.[1,2] Within this catalysis sector, in 2023, global demand for hydrogen reached 97 megatons with production coming mainly from fossil fuels.[3] Given how deeply catalysis is embedded in modern society, and how important hydrogenation is to modern chemical industries, it is important to understand its mechanisms to ensure its continued evolution and uncover new applications in both commercial and research industries.[4–6] Hydrogen spillover (HSPE) refers to the phenomenon in which fundamentally, hydrogen atoms migrate along the surface of a heterogeneous catalyst, typically by the use of spilling over onto a catalyst support for the use of hydrogenation catalysis.[7,8] Similarly, hydrogen atom transfer (HAT) allows for the migration of hydrogen radicals through the use of ligands in homogeneous catalysts.[9] Given the dichotomy of heterogeneous *vs.* homogeneous catalysis which is fundamental to their form as a solid state material *versus* a discrete molecular complex, it is unusual to find a compound that exhibits the behaviors of both.

In our previous work, Rosenberg *et al.* used the stabilization from high mixing entropy to force platinum to alloy into the high-entropy boride (HEB): $Al_{0.2}Nb_{0.2}Pt_{0.2}Ta_{0.2}Ti_{0.2}B_2$. This was the highest-coordinated platinum boride species reported thus far, a remarkable 12-coordinated platinum boride phase.[10] Platinum borides, prior to the discovery of this HEB, were only boron-poor phases with low platinum coordination: Pt_3B_2 (platinum coordinated by 6 boron atoms), PtB (platinum coordinated by 6 boron atoms), and Pt_2B (platinum coordinated by 3 boron atoms).[11–13] The fascination with forming a platinum high-entropy diboride comes from its unique crystal structure of alternating borophene sheets and metal atoms (Fig. 1). Platinum-based catalysts are poisoned by ppm concentrations of sulfur.[14–16] Boron contributes sulfur resistivity for poison-resistant catalysis, allowing it to avoid sulfur poisoning, even at elevated sulfur concentrations, and enabling a longer catalyst lifetime.[17–19] What made $Al_{0.2}Nb_{0.2}Pt_{0.2}Ta_{0.2}Ti_{0.2}B_2$ remarkable was its ability to catalytically reduce 4-nitrothiophenol which contains a thiol group directly functionalized to

[a]Department of Chemistry, University at Albany, State University of New York, Albany, New York, 12222, USA. E-mail: twang3@albany.edu, mtyeung@albany.edu
[b]The RNA Institute, University at Albany, State University of New York, Albany, New York, 12222, USA

† Electronic supplementary information (ESI) available. See DOI: https://doi.org/10.1039/d5qi00311c

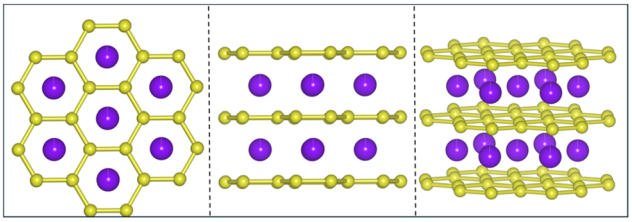

Fig. 1 Atomic representation of the $Al_{0.2}Nb_{0.2}Pt_{0.2}Ta_{0.2}Ti_{0.2}B_2$ hexagonal crystal structured high-entropy boride; the yellow spheres represent the boron atoms, and the purple spheres represent the random distribution of metal atoms Al, Nb, Pt, Ta and Ti.

the substrate. This would have been the worst possible test case for poison-resistant catalysts as the substrate itself is poisonous at ~1000 ppm loadings, far exceeding the sulfur tolerance of previous poison-resistant catalysts. This remarkable tolerance must be derived from the borophene sheets' most important function, that is, shielding platinum from sulfur, while maintaining its high catalytic activity.

High-entropy alloys were first introduced by both Yeh and Cantor who proposed that incorporating five or more principal elements could promote the formation of a single-phase structure.[20,21] The high mixing entropy of the structure's five or more components thermodynamically stabilizes a single solid-phase compound, enabling them to overcome the tendency to separate into individual phases and form a single solid-solution phase at elevated temperatures.[20] Here, the change in Gibbs free energy $\Delta G = \Delta H - T\Delta S$ (where G is Gibbs free energy, H is enthalpy, T is temperature, and S is entropy) where the larger ΔS will cause ΔG to become negative and thus facilitate the spontaneous formation of a high-entropy alloy. The four additional metals that were alloyed with platinum in our HEB were chosen diligently following the Hume-Rothery rules for alloying; all these metals crystalize into diborides, their metallic radii (size) differ by less than 15% from that of platinum, and they have similar electronegativities and counts of valence electrons.[6,22] The Hume-Rothery rules for alloying established a basic elemental scaffold, which was then adjusted to break the Hume-Rothery rules to force platinum into this high-entropy boride. Our previous work had not investigated the mechanism or route for how hydrogenation catalysis occurs. We hypothesize that the HEB follows a hybrid mechanism between the hydrogen spillover effect, as found in heterogeneous catalysis, and hydrogen atom transfer, as found in homogeneous catalysis.[23] Both mechanisms produce mobile hydrogen radicals as the principal reducing agent. In this work, we look to find convincing evidence that the HEB is capable of using a hybrid HSPE/HAT mechanism for its catalytic pathway.

In 1964, Khoobiar reported in his seminal paper that the normally green WO_3 is reduced by H_2 gas to blue H_xWO_3 when in contact with a platinum metal catalyst through simple mixing, thus being the first to establish the possibility of hydrogen spillover.[7,8] This process was later characterized as hydrogen spillover by Boudart *et al.*, which is described as the migration of hydrogen atoms from a hydrogen-rich platinum surface, spilling over to a hydrogen-poor surface and reducing the WO_3.[24] While the exact definition of HSPE is theoretical, the most commonly accepted explanation is that a hydrogen molecule (H_2) attaches to the heterogeneous platinum catalyst, dissociating into atomic hydrogen on the platinum surface, and finally hydrogen spills over from the catalyst onto its support toward the substrate.[25] In addition to the work done by Khoobiar and Boudart on their fundamental contributions to understanding spillover as a concept, progress has continuously been made in applications utilizing spillover for hydrogen storage and advances in catalysis.[25–29] On the other hand, hydrogen atom transfer with homogeneous transition metal catalysts consists of a hydrogen source dissociating on the metal complex, followed by a radical reaction with the coordinated hydrogen.[30–32]

$$\text{L–M} + \frac{1}{2}\text{H}_2 \;\leftrightarrow\; \text{L–M–H}$$

$$\text{L–M–H} + \cdot\text{X} \rightarrow \text{L–M} + \text{H–X}$$

HAT specifically requires the formation of transferable hydrogen radicals from homogeneous catalysts typically in solution. These two reactions will be important to get closer to identifying the actual mechanism that our HEB is using for hydrogenation catalysis. It is important to note that pure hydrogen gas is incapable of performing the HSPE or HAT, as without a catalyst, the hydrogen will not dissociate into mobile hydrogen atoms.[9]

In this work, we investigate whether our HEB catalyst can hydrogenate both WO_3 and 2,2,6,6-tetramethyl-1-piperidinyloxyl (TEMPO) compounds, while comparing to a basic pure platinum catalyst, which can readily hydrogenate these compounds. While we observe the hydrogenation of WO_3 in the traditional gaseous state reaction, we also further investigated performing this reaction in a non-reducible liquid medium. The TEMPO reactions were also examined in the same reaction states. Researchers question whether HSPE can occur in a liquid medium.[25] The non-reducible solution is critical, as otherwise the hydrogen radicals would reduce the solvent. Here, we take a qualitative approach for analyzing the ability of our HEB to hydrogenate WO_3 and TEMPO by observing their prospective color changes after their respective reductions. Furthermore, we show that our HEB catalyst maintains the radical hydrogenation mechanism in poisonous environments by purposely saturating the reaction environment with thiols.

Regardless of whether our HEB exhibits an HSPE or HAT mechanism, the crystallinity and crystal structure are crucial to the hydrogenation reaction.[33–35] Hydrogen needs to have sufficient space and access to bond to platinum; if the crystal facets are not well defined, hydrogen will not be activated and cannot contribute to the catalysis. In this work, we investigate the difference in the synthesis methods of the HEB, comparing the molten aluminum flux growth method with highly defined facets to the arc-melting synthesis, which produces undefined

crystal facets. Here, we show that clear facets along the crystal edge are capable of being catalytically active.

Results and discussion

The high-entropy boride $Al_{0.2}Nb_{0.2}Pt_{0.2}Ta_{0.2}Ti_{0.2}B_2$ is a hybrid catalyst that straddles the division between homogeneous and heterogeneous catalysis. From a heterogeneous catalyst perspective, HEBs are refractory borides that are insoluble in solution which enables their recovery and reuse. From a homogeneous catalyst perspective, the HEB is comprised of borophene sheets that sandwich metal atoms. In effect, the borophene layers serve as shielding ligands and the edges of single crystals would thus resemble a metallocene. This heterogeneous catalyst is comprised of significant extended covalent structures that would provide the protective effect of ligands in homogeneous catalysts while maintaining the recoverability and industrial relevance of heterogeneous catalysts. Here, the covalent network would isolate catalytically active metal centers just like homogeneous catalysts, and the exposed surface of the single crystal facets would perform like anchored homogeneous catalysts but with exceptionally higher stability owing to the refractory nature of heterogeneous catalysts.

To gain a deeper understanding of how the crystal structure, or more specifically the morphology, affects its catalytic activity, we investigated the crystallization of the HEB across synthetic methods. In our previous work, we had prepared the HEB $Al_{0.2}Nb_{0.2}Pt_{0.2}Ta_{0.2}Ti_{0.2}B_2$ by crystallizing it in molten aluminum; this modified flux growth method was adapted from single-crystal growth and thus we would expect to obtain tiny single crystals as the product. Likewise, arc melting from elemental Al, Nb, Pt, Ta, Ti, and B should result in an ingot that upon crushing should result in a poorly faceted sample with random morphology akin to crushed powder. When comparing the arc-melting *vs.* flux growth methods for synthesizing the HEB $Al_{0.2}Nb_{0.2}Pt_{0.2}Ta_{0.2}Ti_{0.2}B_2$, we can see that the flux grown sample is more crystalline, containing abundantly clear facets and numerous hexagonal macrocrystals, which are reflective of its hexagonal microcrystalline structure (Fig. 2). Energy-dispersive X-ray spectroscopy (EDS) was performed on single microcrystals to show the homogeneous distribution of metals on the surface of the crystals (Fig. S1–S3†). The powder X-ray diffraction (pXRD) patterns for both samples confirm the crystal system as MB_2 (AlB_2 type) with the space group (191) *P6/mmm*, while the arc-melted sample has some Al_2O_3 impurities present, which is a result of grinding the HEB ingot into a fine powder using a sapphire mortar and pestle for analysis by pXRD and SEM (Fig. 3).[36]

With the flux grown sample found to be more crystalline, what does this mean for their ability to perform hydrogen spillover on WO_3? To that end, we mixed WO_3 with our catalyst and then performed the hydrogenation with hydrogen gas. The flux grown HEB readily hydrogenates WO_3 in 5% H_2, 95% argon (Fig. 4C), whereas the arc-melted sample was unable to hydrogenate WO_3 under the same gaseous reaction conditions. To confirm that the arc-melted HEB was unable to catalyze WO_3, first the time was increased to 24 hours in 5% H_2, 95% argon (Fig. 4D) and then the environment was changed to 100% H_2 over 24 hours (Fig. 4E). Neither method was successful as the WO_3 was left in its green non-hydrogenated form, whereas the flux grown HEB and platinum readily hydrogenated WO_3 in a dilute hydrogen environment. This exemplifies the necessitation for flux growth of the HEB, giving support to the importance of platinum metallocene-like edges of the crystals needed to drive catalytic activity. The arc-melted HEB

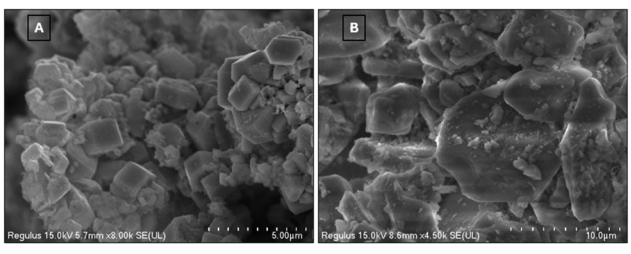

Fig. 2 Scanning electron microscopy images of the different synthesis methods of the HEB $Al_{0.2}Nb_{0.2}Pt_{0.2}Ta_{0.2}Ti_{0.2}B_{0.2}$. (A) Flux growth method, showing its clear and numerous facets. (B) Arc-melting synthesis, showing poorly defined facets.

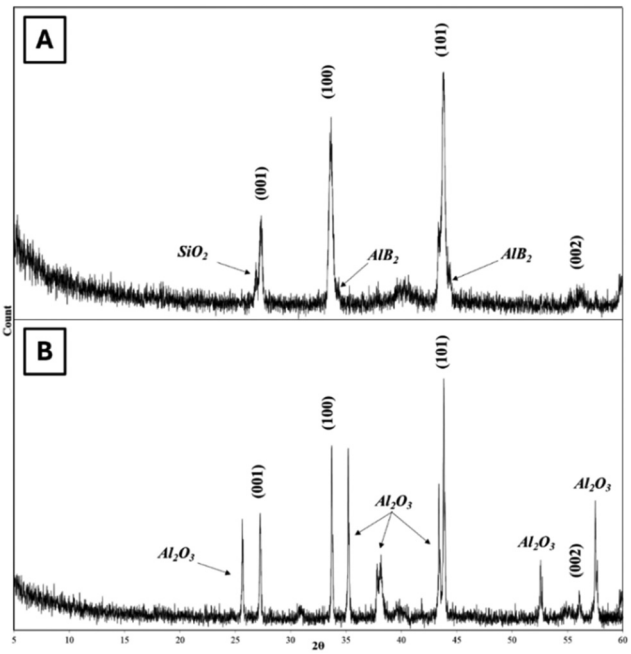

Fig. 3 (A) pXRD pattern of the flux grown HEB $Al_{0.2}Nb_{0.2}Pt_{0.2}Ta_{0.2}Ti_{0.2}B_2$. Note the three sharp peaks of the HEB with their labelled Miller indices indicative of an MB_2 structure, the SiO_2 peaks from grinding the unreacted powder using an agate mortar and pestle, and AlB_2 forming from the aluminum flux. (B) pXRD of the arc-melted HEB $Al_{0.2}Nb_{0.2}Pt_{0.2}Ta_{0.2}Ti_{0.2}B_2$. Note that the same HEB peaks are present, and Al_2O_3 peaks are also prevalent, due to the final polishing of the sample into a fine powder after breaking up the ingot using the synthetic sapphire mortar and pestle.

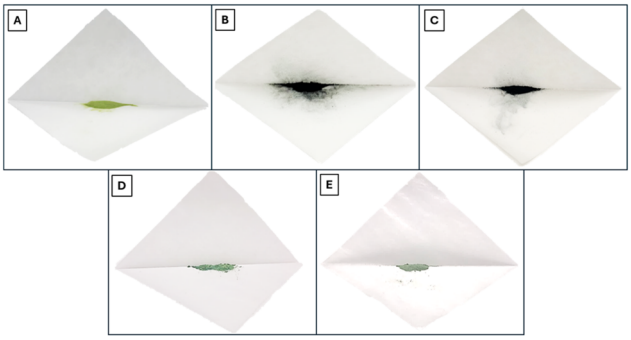

Fig. 4 (A) Unreacted WO_3 powder. (B) WO_3 after hydrogenation with pure platinum powder in the presence of 5% H_2, 95% argon after 1 hour shows H_xWO_3 formation. (C) WO_3 after hydrogenation with the flux grown HEB catalyst in the presence of 5% H_2, 95% argon after 1 hour shows H_xWO_3 formation. (D) WO_3 after exposure to the arc-melted HEB catalyst in the presence of 5% H_2, 95% argon, unreacted after 24 hours shows no reduction. (E) WO_3 after exposure to the arc-melted HEB catalyst in the presence of 100% H_2 shows no reduction after 24 hours.

cannot bind hydrogen with platinum and dissociate or transport hydrogen to the substrate. Here, facet expression around the edges is less pronounced, which can be seen from the SEM images and explained by the observance of size broadening from the pXRD pattern of the flux grown HEB, confirming the existence of smaller crystals.

Given the hybrid nature of $Al_{0.2}Nb_{0.2}Pt_{0.2}Ta_{0.2}Ti_{0.2}B_2$, the potential mechanism for hydrogenation can be viewed from the lens of a homogeneous, hydrogen atom transfer mechanism or a heterogeneous, hydrogen spillover effect mechanism. As the edges of the single crystal particles should resemble a platinum metallocene, each platinum atom can be thought of as an isolated atom surrounded by ligands. In effect, the edges should behave as a platinum complex which is known to release hydrogen radicals.[30] We hypothesize that similar hydrogen atom transfer mechanisms can be explained by Scheme 1. When viewing the mechanism from the lens of a heterogeneous, hydrogen spillover effect mechanism, the borophene sheet separation can be thought of as a pore. Based on the pXRD pattern, we can determine the interlayer spacing between borophene sheets by using the lattice parameters: a = 3.073(2) Å and c = 3.278(1) Å.[10] The [001] Miller indices would represent the d-spacing of the borophene sheets representing the interlayer spacing. We can then subtract the Slater radii of two boron atoms (0.85 Å) to find the true pore size to be 1.578 Å.[37] This is just large enough for hydrogen atoms (1.0 Å in diameter) to access the platinum atom, while being small enough to prevent any other species such as poisonous sulfur (2.0 Å in diameter) from binding to the catalytically active site.[37] From there, the hydrogen dissociates into atomic hydrogen, leaves the "pocket", and then spills over the surface of the particle. It could be argued that within the high-entropy boride particles, the surface serves as the non-reducible support for the entrapped platinum atom (Fig. 5).

Indeed, spillover has been the mechanism in previous attempts at poison-resistant catalysts where the restrictive pore size selectively ensures that atomic hydrogen is the mobile and active species. Yang *et al.* implanted platinum nanoparticles inside zeolite cages with 3 Å pores, and were able to demonstrate sulfur tolerance by sequestering platinum and using spillover hydrogen as the reducing agent.[38] Likewise, Calderone *et al.* encapsulated platinum colloids in nanoporous silica with ~4 Å pores and were able to achieve some degree of sulfur tolerance.[39] Regardless of the mechanism, both HAT and HSPE rely on mobile hydrogen radicals to serve as the principal reducing agent. It could be argued, what makes the HEB sulfur-resistant is that boron's role in the mechanism is more than just a steric shield against sulfur. To confirm whether a boron–hydrogen bond is formed, we exposed the HEB catalyst to H_2 under 1 atm for 24 hours and measured the sample using FTIR, which showed no peak around 2500 cm^{-1}, suggesting that no boron–hydrogen bond is formed in the catalytic process (Fig. S4†).[40] Additionally, the WO_3 samples were analyzed *via* pXRD before and after the reduction to confirm that a hydrogen insertion is taking place rather than forming a suboxide or ordered oxygen vacancies (Fig. S5†).

$$B_{12}Pt + \tfrac{1}{2}H_2 \longrightarrow B_{12}PtH$$
$$B_{12}PtH \rightleftharpoons B_{12}Pt\bullet + H\bullet$$
$$H\bullet + \bullet T \longrightarrow R\text{-}T$$

Scheme 1 The mechanism of hydrogen atom transfer potentially involved in the HEB. The hydrogen gas dissociates onto the platinum complex, followed by a radical attack on the coordinated hydrogen from T (representing a reducible moiety). Note that B_{12} represents the borophene layer as the ligand on platinum.

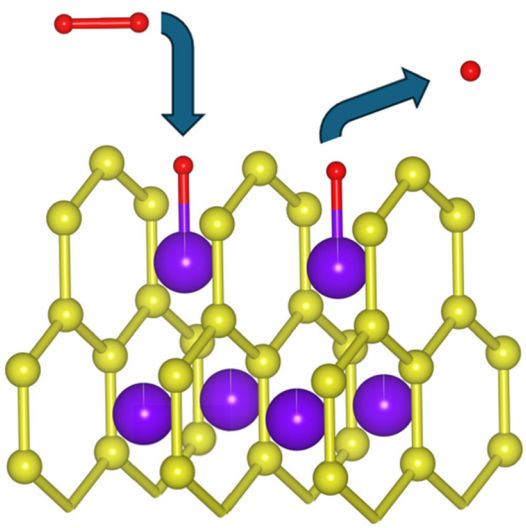

Fig. 5 Potential hydrogen spillover effect on the HEB. The hydrogen gas (red) dissociates, binds to platinum (purple) and spills over along the surface of the particles.

To further study the mechanism and identify the principal reducing agent, we investigated WO_3 and TEMPO reduction in methanol solution under 100% hydrogen gas. Holzapfel *et al.* reported using platinum catalysts to reduce TEMPO, a stable radical solution, *via* a hydrogen spillover pathway.[41] Similar to the WO_3 hydrogenation, the TEMPO reduction results in a color change from its natural amber coloration to a water-white coloration.[41] Both the HSPE and HAT mechanisms produce hydrogen radicals; we use TEMPO as a secondary confirmation of whether our HEB is able to indeed perform hydrogen spillover.[41] The TEMPO compound necessitated a liquid medium, due to its volatility. The possibility of HSPE occurring in solution is still debated, particularly whether a hydrogen radical can transfer and remain stable, even in a non-reducible solution. HSPE occurring in solution is still up for debate, whether it is possible for spillover to occur in solution and whether a hydrogen radical is willing to spillover and be stable in solution, even if the solution is non-reducible. This heterogeneous catalysis was done with a suspended solid solution – WO_3 – and in a dissolved solution – TEMPO. The HEB and platinum catalysts were both able to hydrogenate both WO_3 (Fig. 6D) and TEMPO samples (Fig. 6H). The control HEB $Al_{0.25}Nb_{0.25}Ta_{0.25}Ti_{0.25}B_2$ was used to show that platinum was required to facilitate the hydrogenation catalysis (Fig. 6B and F). Switching from a gaseous environment to a liquid medium meant that the reaction time needed to be increased as the rate of reaction was slowed down significantly; we increased the time from 1 hour to 48 hours. While the HEB was able to readily hydrogenate the samples spiked with benzyl mercaptan, the pure platinum sample, expectedly, was poisoned and was unable to perform its hydrogenation reaction. As expected, the borophene layer acted as a poison-resistant shield, where the pure platinum sample was left vulnerable to sulfur and was inevitably poisoned and deactivated catalytically (Fig. 7).

We believe that our HEB carries out hydrogenation catalysis through a hybrid HAT/HSPE mechanism reflective of its unique crystal structure. When we recreated the seminal hydrogen spillover paper by Khoobiar *et al.* and compared WO_3 hydrogenation between the HEB and pure platinum, both the HEB and platinum metal demonstrated H_xWO_3 formation, suggesting the HSPE mechanism and reinforcing the idea that the mechanism occurs under identical conditions. The reaction with TEMPO helps confirm our suspicions that HAT/HSPE is the preferred mechanism, as both generate hydrogen radicals as the principal reducing agent. While the borophene layer does a great job of protecting the platinum atoms on the edges of the diboride single crystals, while doing this, it is calculated based on the Slater radii that the *d*-spacing between boron atoms is 1.578 Å. This spacing is what prohibits sulfur (2.0 Å) from adhering to platinum, and this also contributes to strong interactions with hydrogen, allowing sufficient room for the hydrogen–platinum bond to form, followed by the dissociation of hydrogen atoms on the surface. Hydrogen, sticking out of the platinum 'pocket', has abundant room for reactions to occur, whether it be through HSPE or HAT mechanisms. In contrast, the catalyst exhibits a HAT-like mechanism in solution. It is generally accepted that for hydrogen spillover to occur, a non-reducible support must be present to allow the hydrogen spillover to occur.[9] This coupled with performing the reactions in methanol solution suggests a more homogeneous catalyst-like mechanism.

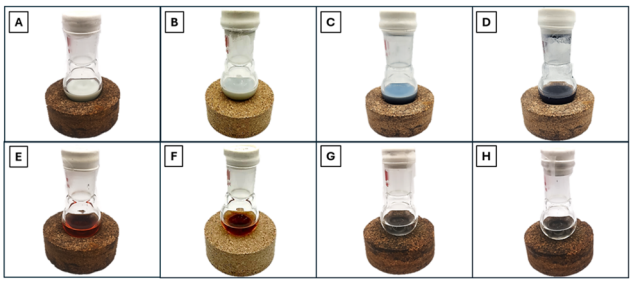

Fig. 6 Hydrogenation reactions of WO_3 and TEMPO under 1 atm H_2 in methanol for 48 hours with constant agitation. (A) WO_3 with no catalyst shows no reduction. (B) WO_3 with the platinum-free HEB $Al_{0.25}Nb_{0.25}Ta_{0.25}Ti_{0.25}B_2$ shows no reduction. (C) WO_3 hydrogenation with the pure platinum catalyst shows reduction. (D) WO_3 hydrogenation with the HEB catalyst shows reduction. (E) TEMPO with no catalyst shows no reduction. (F) TEMPO with the platinum-free HEB $Al_{0.25}Nb_{0.25}Ta_{0.25}Ti_{0.25}B_2$ shows no reduction. (G) TEMPO hydrogenation with the pure platinum metal shows reduction. (H) TEMPO hydrogenation with the HEB catalyst shows reduction.

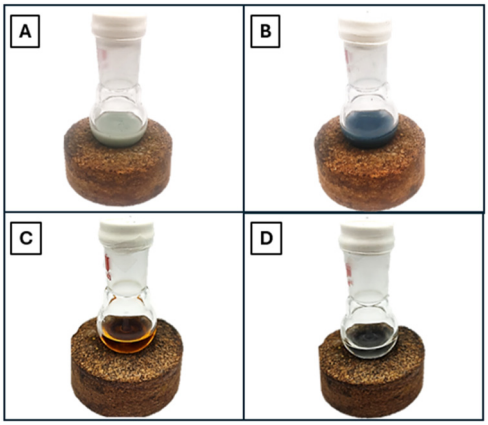

Fig. 7 Comparison of the benzyl mercaptan doped hydrogenation reactions between WO_3 and TEMPO under 1 atm H_2 in methanol for 48 hours. (A) WO_3 hydrogenation reaction with the pure platinum catalyst shows no reduction. (B) WO_3 hydrogenation reaction with the HEB catalyst shows reduction. (C) TEMPO hydrogenation reaction with the pure platinum catalyst shows no reduction. (D) TEMPO hydrogenation reaction with the HEB catalyst shows reduction.

Conclusions

While it is not abundantly clear whether the HEB $Al_{0.2}Nb_{0.2}Pt_{0.2}Ta_{0.2}Ti_{0.2}B_2$ uses the hydrogen spillover effect (HSPE) or the hydrogen atom transfer (HAT) mechanisms as a catalyst in hydrogenation reactions, some valuable insights have been obtained from the work done here; for example, it is

critical that the HEB is synthesized using a flux growth method, and this is pivotal for obtaining clear facets along the crystals, allowing abundant room for platinum to perform the catalysis within the diboride. The heterogeneous hydrogenation reactions of both WO_3 and TEMPO and comparing their successful reactions between the HEB and pure platinum catalyst without a support suggests that the mechanism for the HEB hydrogenation catalysis proceeds through a hybrid HAT/HSPE mechanism. We propose that the mechanism for hydrogenation is a hybrid of the two, where the H_2 binds to the platinum atoms on the facet edges of the HEB and dissociates, and then the radical hydrogens will depart to the substrate.

Future *in situ* and facet-dependent characterization will examine the binding of hydrogen radicals and their exact chemical state in relation to the HEB surface and subsequent hydrogenation of oxides.[42,43] Additionally, theoretical modelling is planned to investigate the facet-dependent catalytic properties of the HEB using DFT calculations.[44] Time-resolved UV-VIS spectroscopic measurements will be conducted *in situ* using an alternative hydrogen source to gather kinetic data.[45]

Author contributions

A. A. R., M. T. Y., and T. W. conceived the idea and analyzed the data. A. A. R. and M. T. Y. wrote the draft manuscript. A. A. R., D. T. L., J. L., Y. Z., J. T. D., M. N. B., and A. K. collected the data. All authors reviewed the results and approved the final version of the manuscript.

Data availability

The data underlying this study are included in the ESI.†

Conflicts of interest

There are no conflicts to declare.

Acknowledgements

The authors thank SUNY Albany for startup funds. This project was supported by innovation funding from the Minerva Center for High-Impact Practices and SUNY System Administration.

References

1 T. Taseska, W. Yu, M. K. Wilsey, C. P. Cox, Z. Meng, S. S. Ngarnim and A. M. Müller, Analysis of the Scale of Global Human Needs and Opportunities for Sustainable Catalytic Technologies, *Top. Catal.*, 2023, **66**, 338–374.
2 R. Catlow, M. Davidson, C. Hardacre and G. J. Hutchings, Catalysis Making the World a Better Place, *Philos. Trans. R. Soc., A*, 2015, **374**, 20150089.
3 Global Hydrogen Review 2024 – Analysis, **https://www.iea.org/reports/global-hydrogen-review-2024**, (accessed 21 March 2025).
4 L. Gausas, S. K. Kristensen, H. Sun, A. Ahrens, B. S. Donslund, A. T. Lindhardt and T. Skrydstrup, Catalytic Hydrogenation of Polyurethanes to Base Chemicals: From Model Systems to Commercial and End-of-Life Polyurethane Materials, *JACS Au*, 2021, **1**, 517–524.
5 I. A. Makaryan and I. V. Sedov, Hydrogenation/Dehydrogenation Catalysts for Hydrogen Storage Systems Based on Liquid Organic Carriers (A Review), *Pet. Chem.*, 2021, **61**, 977–988.
6 A. E. Hughes, N. Haque, S. A. Northey and S. Giddey, Platinum Group Metals: A Review of Resources, Production and Usage with a Focus on Catalysts, *Resources*, 2021, **10**, 93.
7 S. Khoobiar, Particle to Particle Migration of Hydrogen Atoms on Platinum—Alumina Catalysts from Particle to Neighboring Particles, *J. Phys. Chem.*, 1964, **68**, 411–412.
8 D. Bianchi, G. E. E. Gardes, G. M. Pajonk and S. J. Teichner, Hydrogenation of ethylene on alumina after hydrogen spillover, *J. Catal.*, 1975, **38**, 135–146.
9 X.-J. Bai, C. Yang and Z. Tang, Enabling long-distance hydrogen spillover in nonreducible metal-organic frameworks for catalytic reaction, *Nat. Commun.*, 2024, **15**, 6263.
10 A. A. Rosenberg, J. Li, Y. Zhang, J. T. Doane, W. Rice, T. Wang and M. T. Yeung, High-Entropy-Stabilized Platinum Diborides for Poison-Resistant Catalysis, *ChemCatChem*, 2025, **17**, e202401460.
11 G. Akopov, M. T. Yeung and R. B. Kaner, Rediscovering the Crystal Chemistry of Borides, *Adv. Mater.*, 2017, **29**, 1604506.
12 B. Albert and K. Hofmann, in *Handbook of Solid State Chemistry*, John Wiley & Sons, Ltd, 2017, pp. 435–453.
13 B. Albert and H. Hillebrecht, Boron: Elementary Challenge for Experimenters and Theoreticians, *Angew. Chem., Int. Ed.*, 2009, **48**, 8640–8668.
14 S. Ke, L. Qiu, W. Zhao, C. Sun, B. Cui, G. Xu and M. Dou, Understanding of Correlation between Electronic Properties and Sulfur Tolerance of Pt-Based Catalysts for Hydrogen Oxidation, *ACS Appl. Mater. Interfaces*, 2022, **14**, 7768–7778.
15 H. Ning, B. Jiang, L. Yue, Z. Wang, S. Zuo and Q. Wang, Quantitative sulfur poisoning of nanocrystal PtO2/KL-NY and its deactivation mechanism for benzene catalytic oxidation, *Chem. Eng. Sci.*, 2024, **293**, 120086.
16 J. R. Rostrup-Nielsen, in *Progress in Catalyst Deactivation*, ed. J. L. Figueiredo, Springer Netherlands, Dordrecht, 1982, pp. 209–227.
17 C. H. Bartholomew, P. K. Agrawal and J. R. Katzer, in *Advances in Catalysis*, ed. D. D. Eley, H. Pines and P. B. Weisz, Academic Press, 1982, vol. 31, pp. 135–242.
18 W.-J. Wang, H.-X. Li and J.-F. Deng, Boron role on sulfur resistance of amorphous NiB/SiO_2 catalyst poisoned by carbon disulfide in cyclopentadiene hydrogenation, *Appl. Catal., A*, 2000, **203**, 293–300.

19 J. Oudar, Sulfur Adsorption and Poisoning of Metallic Catalysts, *Catal. Rev.*, 1980, **22**, 171–195.
20 M.-H. Tsai and J.-W. Yeh, High-Entropy Alloys: A Critical Review, *Mater. Res. Lett.*, 2014, **2**, 107–123.
21 B. Cantor, I. T. H. Chang, P. Knight and A. J. B. Vincent, Microstructural development in equiatomic multicomponent alloys, *Mater. Sci. Eng., A*, 2004, **375–377**, 213–218.
22 U. Mizutani, in *Surface Properties and Engineering of Complex Intermetallics*, WORLD SCIENTIFIC, 2010, vol. 3, pp. 323–399.
23 W. C. Conner Jr. and J. L. Falconer, Spillover in Heterogeneous Catalysis, *Chem. Rev.*, 1995, **95**, 759–788.
24 R. B. Levy and M. Boudart, The kinetics and mechanism of spillover, *J. Catal.*, 1974, **32**, 304–314.
25 R. Prins, Hydrogen Spillover., Facts and Fiction, *Chem. Rev.*, 2012, **112**, 2714–2738.
26 G. Zhan and H. C. Zeng, Hydrogen spillover through Matryoshka-type (ZIFs@)n−1ZIFs nanocubes, *Nat. Commun.*, 2018, **9**, 3778.
27 S. Wu, K.-Y. Tseng, R. Kato, T.-S. Wu, A. Large, Y.-K. Peng, W. Xiang, H. Fang, J. Mo, I. Wilkinson, Y.-L. Soo, G. Held, K. Suenaga, T. Li, H.-Y. T. Chen and S. C. E. Tsang, Rapid Interchangeable Hydrogen, Hydride, and Proton Species at the Interface of Transition Metal Atom on Oxide Surface, *J. Am. Chem. Soc.*, 2021, **143**, 9105–9112.
28 P. Li, Y. Dong, Y. Ding, H. Zhang, M. Yang and H. Cheng, Effect of hydrogen spillover on the surface of tungsten oxide on hydrogenation of cyclohexene and N-propylcarbazole, *Int. J. Hydrogen Energy*, 2021, **46**, 3945–3953.
29 J. Li, J. Hu, M. Zhang, W. Gou, S. Zhang, Z. Chen, Y. Qu and Y. Ma, A fundamental viewpoint on the hydrogen spillover phenomenon of electrocatalytic hydrogen evolution, *Nat. Commun.*, 2021, **12**, 3502.
30 A. C. Albéniz, P. Espinet, R. López-Fernández and A. Sen, A Warning on the Use of Radical Traps as a Test for Radical Mechanisms: They React with Palladium Hydrido Complexes, *J. Am. Chem. Soc.*, 2002, **124**, 11278–11279.
31 J. M. Mayer, Understanding Hydrogen Atom Transfer: From Bond Strengths to Marcus Theory, *Acc. Chem. Res.*, 2011, **44**, 36–46.
32 L. Wang and J. Xiao, in *Hydrogen Transfer Reactions: Reductions and Beyond*, ed. G. Guillena and D. J. Ramón, Springer International Publishing, Cham, 2016, pp. 205–259.
33 Y. Sun, L. Zhuang, J. Lu, X. Hong and P. Liu, Collapse in Crystalline Structure and Decline in Catalytic Activity of Pt Nanoparticles on Reducing Particle Size to 1 nm, *J. Am. Chem. Soc.*, 2007, **129**, 15465–15467.
34 J. Navarro-Ruiz, J. Audevard, M. Vidal, C. H. Campos, I. Del Rosal, P. Serp and I. C. Gerber, Mechanism of Hydrogen Spillover on Metal-Doped Carbon Materials: Surface Carboxylic Groups Are Key, *ACS Catal.*, 2024, **14**, 7111–7126.
35 M. Chen, B. Wu, J. Yang and N. Zheng, Small Adsorbate-Assisted Shape Control of Pd and Pt Nanocrystals, *Adv. Mater.*, 2012, **24**, 862–879.
36 B. R. Golla, T. Bhandari, A. Mukhopadhyay and B. Basu, in *Ultra-High Temperature Ceramics*, John Wiley & Sons, Ltd, 2014, pp. 316–360.
37 J. C. Slater, Atomic Radii in Crystals, *J. Chem. Phys.*, 1964, **41**, 3199–3204.
38 H. Yang, H. Chen, J. Chen, O. Omotoso and Z. Ring, Shape selective and hydrogen spillover approach in the design of sulfur-tolerant hydrogenation catalysts, *J. Catal.*, 2006, **243**, 36–42.
39 V. R. Calderone, J. Schütz-Widoniak, G. L. Bezemer, G. Bakker, C. Steurs and A. P. Philipse, Design of Colloidal Pt Catalysts Encapsulated by Silica Nano Membranes for Enhanced Stability in H_2S Streams, *Catal. Lett.*, 2010, **137**, 132–140.
40 H. Hagemann, M. Sharma, D. Sethio and L. M. Lawson Daku, Correlating Boron–Hydrogen Stretching Frequencies with Boron–Hydrogen Bond Lengths in Closoboranes: An Approach Using DFT Calculations, *Helv. Chim. Acta*, 2018, **101**, e1700239.
41 N. P. Holzapfel, M. Chagnot, P. S. Abdar, J. R. Paudel, E. J. Crumlin, J. R. McKone and V. Augustyn, Solution-Phase Synthesis of Platinum-Decorated Hydrogen Tungsten Bronzes for Hydrogen Atom Transfer from Oxides to Molecules, *Chem. Mater.*, 2024, **36**, 11684–11696.
42 P. Darapaneni, N. S. Moura, D. Harry, D. A. Cullen, K. M. Dooley and J. A. Dorman, Effect of Moisture on Dopant Segregation in Solid Hosts, *J. Phys. Chem. C*, 2019, **123**, 12234–12241.
43 C. Huck-Iriart, L. Soler, A. Casanovas, C. Marini, J. Prat, J. Llorca and C. Escudero, Unraveling the Chemical State of Cobalt in Co-Based Catalysts during Ethanol Steam Reforming: an in Situ Study by Near Ambient Pressure XPS and XANES, *ACS Catal.*, 2018, **8**, 9625–9636.
44 A. Omoniyi and A. J. R. Hensley, Coverage- and Facet-Dependent Multiscale Modeling of O* and H* Adsorption on Pt Catalytic Nanoparticles, *J. Phys. Chem. C*, 2024, **128**, 7073–7086.
45 F. Zaera, *In situ* and *operando* spectroscopies for the characterization of catalysts and of mechanisms of catalytic reactions, *J. Catal.*, 2021, **404**, 900–910.